FEBS Open Bio 3 (2013) 124–129

journal homepage: www.elsevier.com/locate/febsopenbio

Production of recombinant 1-deoxy-D-xylulose-5-phosphate synthase from *Plasmodium vivax* in *Escherichia coli*☆

Sumit Handa[a], Divya Ramamoorthy[a], Tyler J. Spradling[a], Wayne C. Guida[a], John H. Adams[b], Kestutis G. Bendinskas[c], David J. Merkler[a,*]

[a]Department of Chemistry, University of South Florida, Tampa, FL 33620, USA
[b]Global Health Infectious Disease Research, Department of Global Health, College of Public Health, University of South Florida, Tampa, FL 33612, USA
[c]Department of Chemistry, State University of New York at Oswego, Oswego, NY 13126, USA

ARTICLE INFO

Article history:
Received 12 November 2012
Received in revised form 18 January 2013
Accepted 21 January 2013

Keywords:
Recombinant DXS expression
MEP pathway

ABSTRACT

Humanity is burdened by malaria as millions are infected with this disease. Although advancements have been made in the treatment of malaria, optimism regarding our fight against malaria must be tempered against the problem of drug resistance in the *Plasmodium* parasites causing malaria. New targets are required to overcome the resistance problem. The enzymes of the mevalonate-independent pathway of isoprenoid biosynthesis are targets for the development of novel antimalarial drugs. One enzyme in this pathway, 1-deoxy-D-xylulose-5-phosphate synthase (DXS), catalyzes the conversion of 1-deoxy-D-xylulose-5-phosphate to isopentenylpyrophosphate and dimethylallyl phosphate. We demonstrate the use of a step deletion method to identify and eliminate the putative nuclear-encoded and transit peptides from full length DXS to yield a truncated, active, and soluble form of *Plasmodium vivax* DXS, the DXS catalytic core (DXS_{cc}).

1. Introduction

Malaria is a devastating health problem: approximately 50% of the world's population is at risk of malaria, 216 million cases of malaria were reported in 2010, and over 650,000 people died of malaria in 2010 [1,2]. Unfortunately, the strides being made to combat malaria must be tempered with the growing problems of drug resistance in the parasites that cause malaria and insecticide resistance in the mosquitoes that spread the parasites [2–5]. Malaria is caused by an infection by one of five species of *Plasmodium* protozoans, specifically, *P. falciparum*, *P. vivax*, *P. ovale*, *P. malariae*, and *P. knowlesi* [6,7]. Infection by *P. falciparum* is dominant in Africa, while infection by *P. vivax* is found throughout Asia and the Americas [6,8,9]. Because of the high mortality rate of *P. falciparum* malaria [10], efforts to treat malaria have been targeted largely against *P. falciparum* malaria [11]. However, *P. vivax* malaria is debilitating, can be fatal, and is more widespread and difficult to treat than *P. falciparum* malaria. Arguably, *P. vivax* malaria may be a greater burden to humanity than *P. falciparum* malaria [8,11].

Enzymes involved in type II fatty acid biosynthesis [12], isoprenoid biosynthesis [13], hemozoin biosynthesis [14], and iron sulfur cluster assembly [15] have been identified as potential targets for the development of novel antimalarial drugs. Of these pathways, the enzymes required for biosynthesis of the isoprenoid precursors, isopentenylpyrophosphate (IPP) and dimethylallyl pyrophosphate (DMAPP), are particularly attractive because the plasmodial route to IPP and DMAPP is completely orthogonal to the mammalian biosynthetic route.

IPP and DMAPP are produced in *Plasmodium* from pyruvate and D-glyceraldehyde 3-phosphate (GAP) via a set of seven reactions [16,17]. In man and other mammals, IPP, DMAPP, and the isoprenoids are produced via the canonical mevalonate-dependent pathway defined by Bloch [18], Cornforth [19], Lynen [20], and Popják [21] over 50 years ago. One particularly intriguing target from the mevalonate-independent pathway (MEP) is 1-deoxy-D-xylulose-5-phosphate synthase (DXS). DXS catalyzes the first and rate-determining step of MEP. DXS catalyzes the condensation of pyruvate and D-glyceraldehyde-3-phosphate to 1-deoxy-D-xylulose-5-phosphate (DXP) and CO_2; this reaction being the first- and rate-determining step of MEP [22–24]. Production of recombinant *Plasmodium* DXS in *Escherichia coli* would greatly enhance drug discovery efforts aimed at this enzyme.

We report here on the use of a step wise deletion approach for the successful production of a catalytically active and soluble form of *P.*

* Corresponding author. Department of Chemistry, University of South Florida, 4202 E. Fowler Ave., CHE 205, Tampa, FL 33620-5250, USA. Tel.: +1 813 974 3579; fax: +1 813 974 3203.
E-mail address: merkler@usf.edu (D.J. Merkler).

2211-5463/$36.00
http://dx.doi.org/10.1016/j.fob.2013.01.007

vivax DXS in *E. coli*. This catalytically active form of *P. vivax* DXS does not possess either the signaling or transit peptide and is designated the DXS catalytic core, DXS_{cc}. *P. vivax* DXS_{cc} has been characterized and compared to DXS enzymes from other organisms. We find that the steady-state kinetic parameters and other biochemical features of *P. vivax* DXS_{cc} are consistent with data published for other DXS proteins [25,26].

2. Materials and methods

2.1. Cloning of the P. vivax dxs gene from genomic DNA

The *P. vivax dxs* gene was extracted from strain *Sal*-1 using the following PCR primers: forward primer, 5′-CCTAGGATCCGATGATAATGGGAACTTCCTCT-3′ and reverse primer, 5′-ATCCAAGCTTGTTGGACACCCCTCCTTGCAG-3′. The *BamHI* and the *HindIII* restriction sites are underlined. The PCR product was cloned into the *BamHI* and *HindIII* restriction sites of pET21b(+) to yield the pET21b(+)-vivax-DXS plasmid with a C-terminal His_6 tag. Cloning of the *P. vivax dxs* gene was confirmed by DNA sequencing.

2.2. Cloning of the P. vivax dxs gene and the constructs without the signal peptide and the transit peptide from a codon optimized gene

A synthetic, codon optimized *P. vivax dxs* gene with 5′-*NdeI* and 3′-HindIII restriction sites in a pUC57 vector was obtained from Genscript. The full length *dxs* gene was excised from pUC57 vector and cloned into *NdeI* and *HindIII* restriction sites of pET21b(+) vector with a C-terminal His_6 tag to yield the vector SH-1. Genes that would yield DXS proteins truncated at the N-terminus were SH-2, SH-3, SH-4, SH-5, SH-6, SH-7, SH-8, and SH-9 (N-terminal deletion of Δ210, Δ245, Δ252, Δ272, Δ303, Δ347, Δ357, and Δ395 amino acids, respectively). These were constructed by PCR extraction from the codon optimized *P. vivax dxs* gene and cloned into *NdeI* and *XhoI* restriction sites of pET28a(+) vector with N-terminal His_6 tag.

2.3. Overexpression of full length and truncated P. vivax DXS proteins in E. coli

Both full length and truncated *P. vivax* DXS proteins were expressed in *E. coli* BL-21 B(DE3) or Rosetta B(DE3) cells. A fresh colony of *E. coli* containing the appropriate plasmid was cultured at 37 °C in LB broth containing 100 μg/mL ampicillin for SH-1 and 50 μg/mL kanamycin for SH-2 to SH-9 supplemented with 0.8% glucose and 25 mM potassium phosphate at pH 7.2. The cultures were grown for 2–3 h until the OD_{600} reached 0.3, then diluted 100-fold, incubated at 37 °C until the OD_{600} reached 0.6, and then cooled to 25 °C. Expression was induced by the addition of 0.5 mM isopropyl β-D-1-thiogalactopyranoside (IPTG), incubated for 5–6 h with shaking, the cells harvested by centrifugation, and the cell pellets stored at −80 °C.

2.4. DXS and DXR purification by Ni-NTA affinity chromatography

Cells were thawed and all the purification steps were performed at 4 °C. Cells were resuspended in the binding buffer (20 mM Tris pH 7.5, 500 mM NaCl, 20 mM imidazole, and 10 mM BME) supplemented with 1 mM PMSF, 4 μg/mL leupeptin, 2 μg/mL pepstatin, sonicated, and centrifuged at 16,000 × *g* for 20 min. The supernatant from the cell lysate was applied to the Ni-NTA resin (1.5 cm × 5 cm, equilibrated with the binding buffer) at a rate of 1 mL/min and the non-bound proteins were eluted from the column by washing with 5 column volumes of the binding buffer followed by 20 column volumes of the wash buffer (20 mM Tris pH 7.5, 500 mM NaCl, 60 mM imidazole, and 10 mM BME. DXS SH-1 and SH-2 were eluted using elution buffer (20 mM Tris pH 7.5, 500 mM NaCl, 250 mM imidazole, and 10 mm BME),

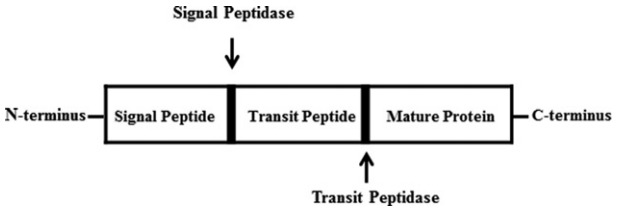

Fig. 1. Schematic diagram of the nuclear-encoded bipartite pre-sequence responsible for apicoplast targeting in *Plasmodium* species.

fractions containing active protein were combined and the protein concentrated for size exclusion chromatography. The truncated DXS protein, DXS SH-2, will be referred to as the DXS catalytic core, DXS_{cc}. Additional details of our experimental methods and the materials can be found in the Supplementary material .

3. Results

3.1. Expression of full length P. vivax DXS using genomic DNA

The expression of proteins from *Plasmodium* in *E. coli* has always been difficult, even more so for proteins targeted to the apicoplast. This problem arises from the differences in codon bias between *E. coli* and *Plasmodium* species [27,28] and from the N-terminal bipartite targeting sequence of apicoplast proteins (Fig. 1). The enzymes of the MEP are located in lumen of the apicoplast [29]; thus, such enzymes from *Plasmodium* are difficult to express in *E. coli*. Not surprisingly, only two MEP enzymes from *Plasmodium* have been expressed in *E. coli*: DXR [30] and 2-*C*-methyl-D-erythritol 2,4-cyclodiphosphate synthase [31]. Both were from *P. falciparum* and were expressed with the N-terminal amino acids deleted from a putative catalytic core. None of MEP enzymes from *P. vivax* have been expressed in *E. coli*, to date.

The open reading frame corresponding for the full length *dxs* gene was isolated from *P. vivax* genomic DNA by PCR (Fig. S1). Expression of full length *P. vivax* DXS in *E. coli* using the *dxs* gene isolated from genomic DNA was first performed as a proof of concept. A final yield of 40 μg of partially purified *P. vivax* DXS per liter of culture from BL-21 cells and 80 μg per liter of culture using Rosetta B(DE3) cell line was obtained. Full length *P. vivax* DXS was active and exhibited a specific activity of 1.2 ± 0.1 μmol/min/mg.

3.2. Expression of full length P. vivax DXS using a synthetic codon optimized dxs gene

The expression of low levels of full length, active *P. vivax* DXS *in E. coli* using the genomic *dxs* gene was encouraging. A synthetic *P. vivax dxs* gene codon optimized for *E. coli* expression was prepared to improve upon the low expression yield. Expression yields of full *P. vivax* DXS_{cc} from *E. coli* improved to ~1.5 mg/L of culture when using the codon optimized gene, but a low molecular weight protein contaminant was always present with the full length DXS (Fig. 2). We varied an array of experimental parameters, including induction temperature, induction time, IPTG concentration, and protease inhibitor combinations, but were unable to eliminate the low molecular weight contaminant from full length *P. vivax* DXS.

3.3. Expression and purification of P. vivax DXS_{cc}

Expression of full length *P. vivax* DXS in *E. coli* using the synthetic *dxs* gene was complicated by the presence low molecular weight protein (Fig. 2). This low molecular weight contaminant is, most likely, a truncated form of DXS resulting from the proteolytic removal of the

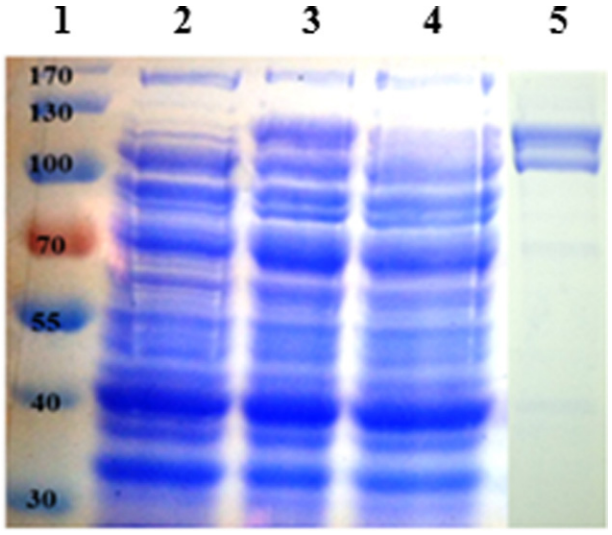

Fig. 2. SDS–PAGE analysis of nuclear encoded full length *P. vivax* DXS purification. Molecular weight markers (with molecular weight values highlighted inside the bands) (lane 1), uninduced control (lane 2), cell lysate (lane 3), flow through from affinity chromatography (lane 4), and purified full length *P. vivax* DXS (lane 5).

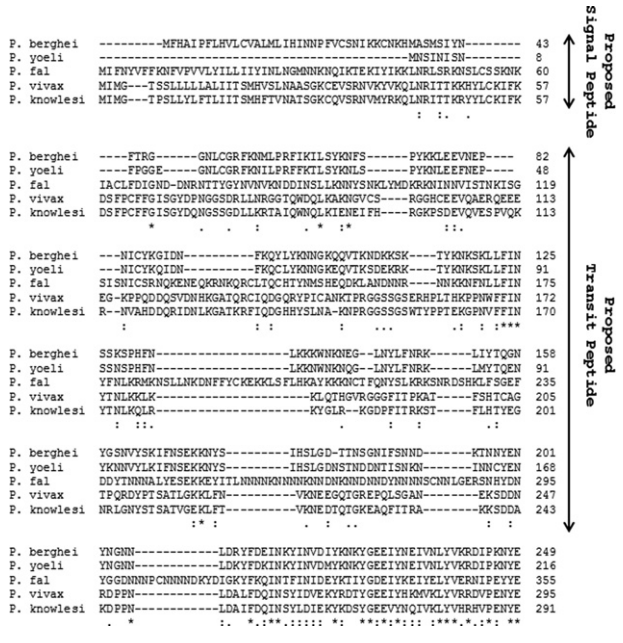

Fig. 3. Sequence comparison of the N-terminal regions of DXS from *P. berghei*, *P. yoeli*, *P. falciparum*, *P. vivax*, and *P. knowlesi*. The alignments were constructed using Clustal W2 with the asterisk (*) indicating a fully conserved residue, the colon (:) indicating conservation between residues of strongly similar properties, and a period (.) indicating conservation between residues of weakly similar properties. P. fal = *P. falciparum*.

N-terminal bipartite pre-sequence by an *E. coli* protease. Our solution to this problem was to directly express the *P. vivax* DXS_{cc} in *E. coli* by eliminating the bipartite targeting peptide from the optimized full length *dxs* gene. Bioinformatic tools to predict the signal peptide generally work well and predicted a signal peptide compromising the first 23–30 amino acids in full length *P. vivax* DXS (Table 1).

The accurate prediction of the transit peptide, which serves in the movement of a protein into the lumen of the apicoplast, is not possible because transit peptides vary considerably in length and sequence. In addition, the cleavage site to remove the transit peptide from the mature protein apicoplast is not well understood. Thus, there is no consensus sequence for the transit peptide.

In order to express the soluble and active *P. vivax* DXS_{cc} without the signaling and transit peptides, sequences of *E. coli*, *Deinococcus radiodurans*, and *P. vivax* DXS were compared (Fig. S2). Based on sequence similarities between the DXS enzymes from *E. coli* and *D. radiodurans*, we designed clones SH-7 to SH-9 to eliminate large sections of the N-terminus from full length enzyme. A similar strategy was used for the expression of active forms of *P. falciparum* DXR and IspF in *E. coli* [30,31]. Clones SH-7, SH-8, and SH-9 yielded only microgram levels of soluble, but inactive protein per liter of culture medium.

DXS sequences from five different species of *Plasmodium* species were aligned to better capture the nature of the transit peptide. This comparison revealed little homology in the first 200 N-terminal amino acids; highlighting the difficulty in predicting the transit peptide of *P. vivax* DXS. Given the paucity of guidance from the sequence comparisons on how to best design a gene coding only for DXS_{cc}, we generated a series of clones, each with a progressively longer N-terminal deletion in the final *P. vivax* DXS-derived protein (Fig. S3). This step deletion approach ultimately led to clone SH-2, with an N-terminal deletion of the first 210 amino acids. Expression of the protein derived from SH-2, DXS_{cc}, lead to a soluble, homogenous, and active enzyme in good yield when expressed in *E. coli*. All the other truncated DXS proteins discussed herein produced microgram quantities of soluble, but inactive protein upon expression in *E. coli*.

An investigation of the transit peptide for the *P. falciparum* acyl carrier protein showed that the transit peptide is disordered or adopts a low occupancy helix [32]. Thus, one validation of the predicted transit peptide sequence for *P. vivax* DXS comes from the calculation of sequence entropy for residues 1–250 using DisEMBL [33]. Analysis of the sequence entropy indicated that residues from 1 to 250 are highly disordered (Fig. S4), providing further evidence that the transit peptide for *P. vivax* DXS is defined within the N-terminal 250 amino acids of the full length protein. Since the signal peptide is, most likely, encompassed by the first ~25 amino acids (Table 1), we propose that the transit peptide of full length *P. vivax* DXS extends from about residue 30 to about residue 250 (Fig. 3).

Nickel affinity chromatography was used as a first step in the purification, followed by size exclusion chromatography (Fig. 4(A)). Two major protein peaks were observed in the size exclusion chromatogram. The first peak, representing a protein with a molecular weight corresponding to the DXS_{cc} tetramer or high molecular weight aggregates, exhibits little to no DXS activity. The second peak, representing a protein with a molecular weight of the DXS_{cc} dimer, has relatively high DXS activity (Fig. 4(B) and (C)). The final *P. vivax* DXS_{cc} preparation, obtained using nickel affinity and size-exclusion chromatography, was >99% pure, as judged by SDS–PAGE and Western blot analysis (using anti-His_6 antibody). The final yield of dimeric *P. vivax* DXS_{cc} was approximately 30%, yielding 1 mg/L of enzyme per liter of *E. coli* culture (Table 2).

3.4. Characterization of *P. vivax* DXS_{cc}: pH optimum, molecular weight, and Mg(II) stoichiometry

At saturating concentrations of pyruvate and GAP, a pH optimum of 7–7.5 was determined for *P. vivax* DXS_{cc} (Fig. S5). The pH optimum for *P. vivax* DXS_{cc} is comparable to the values reported for DXS from *Rhodobacter capsulatus* (7.0) [34] and *Agrobacterium tumefaciens* (8.0) [26].

The molecular mass of active *P. vivax* DXS_{cc} estimated by gel filtration chromatography under non-denaturing conditions was 260 kDa (Fig. S6) while the molecular weight of the enzyme estimated by SDS–PAGE analysis was 115 kDa (Fig. 4(C)). These data suggest the *P. vivax* DXS_{cc} exists as a homodimer. DXS from *D. radiodurans* and *R. capsulatus* have been reported to exist as dimers, as well [24,34]. MALDI-MS was further used to confirm the molecular weight of the

Table 1.
Predicted cleavage site between signal and transit peptides.

Software used	N-terminal sequence (cleavage site highlighted)	Expected length
SignalP	MIMGTSSLLLLLALIITSMHVSLN**AA** SGKCEV	25 amino acids
PSORT	MIMGTSSLLLLLALIITSMHVSLNAASGK**CE** V	30 amino acids
PATS	MIMGTSSLLLLLALIITSMHVS**LN** AASGKCEV	23 amino acids
PlasmoAP	MIMGTSSLLLLLALIITSMHVSLN**AA** SGKCEV	25 amino acids

Table 2.
Purification of recombinant *P. vivax* DXS_{cc} from *E. coli*.[a]

Step	Total protein (mg)	Total units (μmol/min)	Specific activity (units/mg)	Fold purification	Yield[b] (%)
Ni(II) affinity chromatography	15	122	8.1	1	100
Size-exclusion chromatography	5.0	97	19.3	2.4	80

[a] We could not accurately measure the total units of DXS_{cc} activity in the *E. coli* cell lysate due to high levels of background NADPH oxidation activity.
[b] The overall yield of DXS_{cc} was approximately 30%, based on our imprecise measurements of DXS_{cc} activity in the *E. coli* cell lysates.

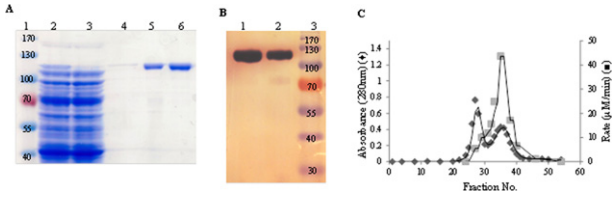

Fig. 4. The purification of *P. vivax* DXS_{cc}. (A) SDS–PAGE analysis of the DXS_{cc} purification. (A) Molecular weight markers (with molecular weight values highlighted inside the bands) (lane 1), cell lysate (lane 2), flow through from affinity chromatography (lane 3), wash (lane 4), elution from the affinity chromatography (lane 5), and purified DXS_{cc} after gel filtration chromatography (lane 6). (B) Western blot analysis of DXS_{cc} using an anti-His_6 antibody. Protein after gel filtration chromatography (lane 1), protein after affinity purification (lane 2), and molecular weight markers (with molecular weight values highlighted inside the bands) (lane 3). (C) Gel filtration profile of *P. vivax* DXS_{cc} during purification.

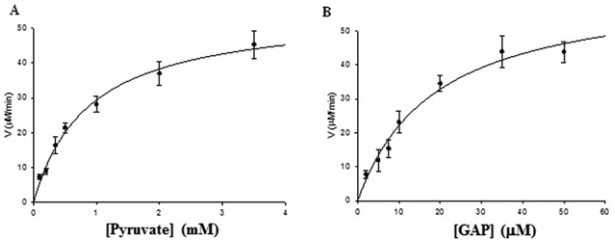

Fig. 5. Steady-state kinetic analysis of *P. vivax* DXS_{cc} for pyruvate (A) and GAP (B) at constant, fixed, and saturating concentration of the other substrate.

monomeric unit. The results of MALDI-MS analysis showed peaks for M, M/2, and 2M peak with the highest intensity observed for the M peak (Fig. S7), and the molecular weight for the M peak corresponding to 103,822 Da with an accuracy of 0.1% (99 Da from the theoretical 103,921 Da).

DXS catalysis requires thiamin pyrophosphate (TPP) to transfer an acetyl unit from pyruvate to GAP in forming DXP. TPP is observed in the crystal structures of both *E. coli* DXS and *D. radiodurans* DXS [24]. Like other TPP-dependent enzymes, DXS also requires a divalent metal ion for catalysis. DXS from *A. tumefaciens* [26], *R. capsulatus* [34], *Streptomyces* [35], and *Mycobacterium tuberculosis* [36], require Mg(II) or Mn(II) for maximum activity.

We found that *P. vivax* DXS_{cc} was completely active even in the absence of any exogenously added TPP or divalent metal ion to the assay solutions or to any of the buffers employed during the purification of the enzyme (data not shown). These data suggest that *P. vivax* DXS_{cc} binds both TPP and metal with relatively high affinity and both were acquired from the culture medium. In order to test the activity of DXS_{cc} in the absence of TPP and metal, the protein was dialyzed against EDTA to remove the bound cofactors. DXS_{cc} was completely active after exhaustive dialysis against EDTA. Incubation of the enzyme with acidic, saturated ammonium sulfate (pH 3.5) lead to the complete removal of TPP, with high recovery of activity upon reconstitution with TPP (Fig. S8). However, the required metal ion remained bound to the enzyme as added Mg(II) had no effect on reconstitution of DXS_{cc} activity.

Preparation of metal-free DXS_{cc} proved difficult as exhaustive dialysis against EDTA in pH 7.0 buffer resulted in completely active enzyme. Incubation of the enzyme with saturated ammonium sulfate and 5.0 mM EDTA at pH 3.5 led to the complete loss of DXS_{cc} activity, with only a 25% recovery of activity upon the addition of Mg(II). Inductively coupled plasma resonance mass spectrometry (ICP-MS) was then used to quantify the amount of Mg(II) in DXS_{cc}. Molar ratio of Mg(II) to DXS was found out to be 0.97 ± 0.01. These results suggest that Mg(II) may serve both a structural and catalytic role in DXS_{cc}, that Mg(II) is bound to DXS_{cc} with a higher affinity than TPP, and that the bound Mg(II) with another divalent metal might be achieved only by culturing the *P. vivax* DXS_{cc}-expressing *E. coli* cells in minimal media supplemented with a divalent metal ion of interest.

3.5. *Kinetic characterization of P. vivax* DXS_{cc}

Steady state kinetic parameters for pyruvate and GAP for *P. vivax* DXS_{cc} were calculated using the DXS–DXR coupled assay (Fig. 5). The steady-state kinetic parameters for DXS_{cc} were comparable to DXS from other bacterial species [39,40,50]. The relatively small differences in the steady-state kinetic parameter for *P. vivax* DXS_{cc} when compared to similar values for DXS *R. capsulatus* and *A. tumefaciens*, may result from the different pH optima of the enzyme from these organisms (Table 3). β-Fluoropyruvate (F-Pyr), a pyruvate analog and a known competitive inhibitor of DXS [25] was used to further characterize *P. vivax* DXS_{cc}. F-Pyr was competitive with respect to pyruvate with a K_i value of 200 ± 100 μM (Fig. 6), a value lower than the K_i of 1.0 ± 0.1 mM reported for DXS from *R. capsulatus* [25].

In conclusion, we report here on the successful expression of a soluble and catalytically active form of *P. vivax* 1-deoxy-D-xylulose-5-phosphate synthase in *E. coli*. *P. vivax* DXS_{cc} exists as a homodimer, contains one-bound Mg(II) per enzyme molecule, and exhibits

Table 3
Comparison of steady state kinetic constants for pyruvate and GAP.

Organism	Pyruvate			GAP			Comment
	K_m (μM)	k_{cat} (s^{-1})	k_{cat}/K_m (M^{-1} s^{-1})	K_m (μM)	k_{cat} (s^{-1})	k_{cat}/K_m (M^{-1} s^{-1})	
P. vivax [a, b]	870 ± 110	9.5 ± 0.5	1.1 × 10^4	19 ± 4	11 ± 0.9	5.7 × 10^5	This study
E. coli	49 ± 8.0	2.6 ± 0.11	5.3 × 10^4	24 ± 1.7	2.6 ± 0.11	1.1 × 10^5	[37]
R. capsulatus	440 ± 50	1.9 ± 0.1	4.3 × 10^3	68 ± 1	1.9 ± 0.1	2.8 × 10^4	[25]
A. tumefaciens [c]	40	27	6.7 × 10^5	23	27	1.2 × 10^6	[26]

[a] For *P. vivax* DXS_{cc}, the apparent kinetic constants for pyruvate were measured by varying the initial concentration of pyruvate at 0.1 mM GAP.
[b] For *P. vivax* DXS_{cc}, the apparent kinetic constants for GAP were measured by varying the initial concentration of GAP at 4.0 mM pyruvate.
[c] No error analysis was reported for the kinetic constants measured for *A. tumefaciens* DXS.

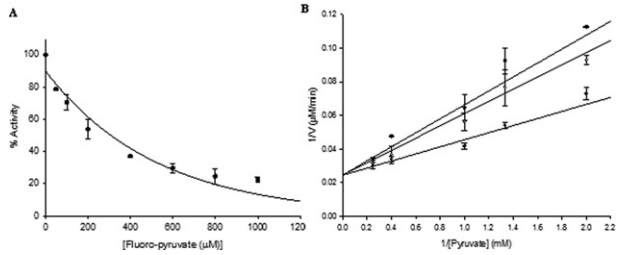

Fig. 6. The inhibition of *P. vivax* DXS_{cc} by β-fluoropyruvate. (A) Inhibition of *P. vivax* DXS by β-fluoropyruvate (F-Pyr) at constant fixed concentrations of pyruvate and GAP. (B) Double reciprocal analysis of initial velocities of DXS inhibition by F-Pyr at different fixed concentration of pyruvate. The kinetic analysis was performed at following concentration of F-Pyr: 0 μM (•), 150 μM (o), and 200 μM (▼), and the initial concentration of GAP was fixed at 0.5 mM.

steady-state kinetic constants similar to other DXS enzymes. Apo-DXS_{cc} is inactive and insoluble suggesting that the bound Mg(II) has both a catalytic and structural role in the enzyme. We also provide some insight concerning the bipartite pre-sequence N-terminus to the mature catalytic core of *P. vivax* DXS. While not conclusive, our data suggest that the bipartite pre-sequence spans from amino acid 1 to ~250 in the full length protein. We propose that the first ~25 amino acids represent the signal peptide while amino acids ~25 to ~250 represent the transit peptide. A proposed length of ~225 amino acids for transit peptide of *P. vivax* DXS is within the range reported for the transit peptides of other proteins characterized from *Plasmodium* (Table S1). The results presented herein will foster the development of DXS inhibitors to treat *P. vivax* malaria and provide a better understanding of the mechanisms used in *Plasmodium* for the transit of proteins coded in the nucleus to the lumen of the apicoplast.

Acknowledgments

This research was supported in part by a seed grant from the Florida Center of Excellence for Biomolecular Identification and Targeted (FCoE-BITT) to D.J.M. and W.C.G., an International Travel Grant from the University of South Florida for a preliminary presentation of this work at IUBMB & FEBS Sevilla 2012 (poster P 15–17) to D.J.M., and a Graduate Multidisciplinary Scholar (GMS) award from FCoE-BITT to S.H. The authors would like to thank Dr. Zachary Atlas (Department of Geology, University of South Florida) for his assistance.

Appendix A. Supplementary material

Supplementary material associated with this article can be found, in the online version, at doi:10.1016/j.fob.2013.01.007.

References

[1] World Health Organization (WHO), World Malaria Report 2011. Available from: <www.who.int/malaria/world_malaria_report_2011/en/>.
[2] Murray C.J.L., Rosenfeld L.C., Lim S.S., Andrews K.G., Foreman K.J., Haring D. et al. (2012) Global malaria mortality between 1980 and 2010: a systemic analysis. Lancet. 379, 413–431.
[3] Schlitzer M. (2007) Malaria chemotherapeutics part I: history of antimalarial drug development, currently used therapeutics, and drugs in clinical development. Chem. Med. Chem. 2, 944–986.
[4] Petersen I., Eastman R., Lanzer M. (2011) Drug-resistant malaria: molecular mechanisms and implications for public health. FEBS Lett. 585, 1551–1562.
[5] Enayati A., Hemingway J. (2010) Malarial management: past, present, and future. Annu. Rev. Entomol. 55, 569–591.
[6] Garcia L.S. (2010) Malaria. Clin. Lab. Med. 30, 93–129.
[7] Collins W.E. (2012) *Plasmodium knowlesi* a malaria parasite of monkeys and humans. Annu. Rev. Entomol. 57, 107–121.
[8] Mendis K., Sina B., Marchesini P., Carter R. (2001) The neglected burden of *Plasmodium vivax* malaria. Am. J. Trop. Med. Hyg. 64(Suppl. 1–2), 97–106.
[9] Gething P.W., Elyazar I.R.F., Moyes C.L., Smith D.L., Battle K.E., Guerra C.A. et al. (2012) A long neglected world malaria map: *Plasmodium vivax* endemicity in 2010. PLoS Negl. Trop. Dis. 6, e1814.
[10] Trape J.-F., Rogier C. (1996) Combating malaria morbidity and mortality by reducing transmission. Parasitol. Today. 12, 236–240.
[11] Carlton J.M., Sina B.J., Adams J.H. (2011) Why is *Plasmodium vivax* a neglected tropical disease? PLoS Negl. Trop. Dis. 5, e1160.
[12] Waller R.F., Ralph S.A., Reed M.B., Su V., Douglas J.D., Minnikin D.E. et al. (2003) A type II pathway for fatty acid biosynthesis presents drug targets in *Plasmodium falciparum*. Antimicrob. Agents Chemother. 47, 297–301.
[13] Yeh E., DeRisi J.L. (2011) Chemical rescue of malarial parasites lacking an apicoplast defines organelle function in blood-stage *Plasmodium falciparum*. PLoS Biol. 9, e1001138.
[14] Egan T.J., Marques H.M. (1999) The role of haem in the activity of chloroquine and related antimalarial drugs. Coord. Chem. Rev. 19, 493–517.
[15] Mather M.W., Henry K.W., Vaidya A.B. (2007) Mitochondrial drug targets in apicomplexan parasites. Curr. Drug Targets. 8, 49–60.
[16] Gräwert T., Groll M., Rohdich F., Bacher A., Eisenreich W. (2011) Biochemistry of the non-mevalonate isoprenoid pathway. Cell. Mol. Life Sci. 68, 3797–3814.
[17] Hunter W.N. (2011) Isoprenoid precursor biosynthesis offers potential targets for drug discover against diseases caused by apicomplexan parasites. Curr. Top. Med. Chem. 11, 2048–2059.
[18] Bloch K. (1962) The biological synthesis of cholesterol. Science. 150, 19–28.
[19] Conforth J.W. (1959) Biosynthesis of fatty acids and cholesterol considered as chemical processes. J. Lipid Res. 1, 3–28.
[20] Lynen F. (1961) Biosynthesis of saturated fatty acids. Fed. Proc. 20, 941–951.
[21] Popák G. (1958) Biosynthesis of cholesterol and related substances. Annu. Rev. Biochem. 27, 533–560.
[22] Lois L.M., Campos N., Putra S.R., Danielsen K., Rohmer M., Boronat A. (1998) Cloning and characterization of a gene from *Esherichia coli* encoding a transketolase-like enzyme that catalyzes the synthesis of D-1-deoxyxylulose 5-phosphate, a common precursor for isoprenoid, thiamin, and pyridoxol biosynthesis. Proc. Natl. Acad. Sci. USA. 95, 2105–2110.
[23] Estévez J.M., Cantero A., Reindl A., Reichler S., León P (2001) 1-Deoxy-D-xylulose phosphate synthase, a limiting enzyme for plastidic isoprenoid biosynthesis in plants. J. Biol. Chem. 276, 22901–22909.
[24] Xiang S., Usunow G., Lange G., Busch M., Tong L. (2007) Crystal structure of 1-deoxy-D-xylulose 5-phosphate synthase, a crucial enzyme for isoprenoid biosynthesis. J. Biol. Chem. 282, 2676–2682.
[25] Eubanks L.M., Poulter C.D. (2003) *Rhodobacter capsulatus* 1-deoxy-D-xylulose5-phosphate synthase: steady-state kinetics and substrate binding. Biochemistry. 42, 1140–1149.
[26] Lee J.-K., Oh D.-K., Kim S.-Y. (2007) Cloning and characterization of the *dxs* gene, encoding 1-deoxy-D-xylulose 5-phosphate synthase from *Agrobacterium tumefaciens*, and its overexpression in *Agrobacterium tumefaciens*. J. Biotechnol. 128, 555–566.
[27] Saul A., Battistutta D. (1988) Codon usage in *Plasmodium falciparum*. Mol. Biochem. Parasitol. 27, 35–42.
[28] Chen N., Cheng Q. (1999) Codon usage in *Plasmodium vivax* nuclear genes. Int. J. Parasitol. 29, 445–449.
[29] Lim L., McFadden G.I. (2010) The evolution, metabolism and functions of the apicoplast. Philos. Trans. R. Lond. B Biol. Sci. 365, 749–763.
[30] Jomaa H., Wiesner J., Sanderbrand S., Altincicek B., Weidemeyer C., Hintz M. et al. (1999) Inhibitors of the nonmevalonate pathway of isoprenoid biosynthesis as

antimalarial drugs. Science. 285, 1573–1576.
[31] Rohdich F., Eisenreich W., Wungsintaweekul J., Hecht S., Schuhr C.A., Bacher A. (2001) Biosythesis of terpenoids. 2-*C*-methyl-D-erythritol 2,4-cyclodiphosphate synthase (IspF) from *Plasmodium falciparum*. Eur. J. Biochem. 268, 3190–3197.
[32] Gallagher J.R., Matthews K.A., Prigge S.T. (2011) *Plasmodium falciparum* apicoplast transit peptides are unstructured *in vitro* and during apicoplast import. Traffic. 12, 1124–1138.
[33] Linding R., Jensen L.J., Diella F., Bork P., Gibson T.J., Russell R.B. (2003) Protein disorder prediction: implications for structural proteomics. Structure. 11, 1453–1459.
[34] Hahn F.M., Eubanks L.M., Testa C.A., Blagg B.S.J., Baker J.A., Poulter C.D. (2001) 1-Deoxy-D-xylulose 5-phosphate synthase, the gene product of open reading frame (ORF) 2816 and ORF 2895 in *Rhodobacter capsulatus*. J. Bacteriol. 183, 1–11.
[35] Kuzuyama T., Takagi M., Takahashi S., Seto H. (2000) Cloning and characterization of 1-deoxy-D-xylulose 5-phosphate synthase from *Streptomyces* sp. Strain CL190, which uses both the mevalonate and nonmevalonate pathways for isopentenyl diphosphate biosynthesis. J. Bacteriol. 182, 891–897.
[36] Bailey A.M., Mahapatra S., Brennan P.J., Crick D.C. (2002) Identification, cloning, purification, and enzymatic characterization of *Mycobacterium tuberculosis* 1-deoxy-D-xylulose 5-phosphate synthase. Glycobiology. 12, 813–820.
[37] Brammer J.A, Smith J.M, Wade H, Meyers C.F (2011) 1-Deoxy-D-xylulose 5-phosphate synthase catalyzes a novel random sequential mechanism. J. Biol. chem. 286, 36522–36531.